7424 *Inorg. Chem.* **2010**, *49*, 7424–7434
DOI: 10.1021/ic100749k

Inorganic Chemistry
Article

Syntheses and Magnetostructural Investigations on Kuratowski-Type Homo- and Heteropentanuclear Coordination Compounds $[MZn_4Cl_4(L)_6]$ (M^{II} = Zn, Fe, Co, Ni, or Cu; L = 5,6-Dimethyl-1,2,3-benzotriazolate) Represented by the Nonplanar $K_{3,3}$ Graph

Shyam Biswas,[†] Markus Tonigold,[†] Manfred Speldrich,[‡] Paul Kögerler,[‡] Matthias Weil,[§] and Dirk Volkmer*,[†]

[†]*Institute of Inorganic Chemistry II, Materials and Catalysis, Ulm University, Albert-Einstein-Allee 11, D-89081 Ulm, Germany,* [‡]*Institute of Inorganic Chemistry, RWTH Aachen University, D-52074 Aachen, Germany, and* [§]*Institute for Chemical Technologies and Analytics, Division of Structural Chemistry, Vienna University of Technology, Getreidemarkt 9/164-SC, A-1060 Vienna, Austria*

Received April 19, 2010

Homo- and heteropentanuclear coordination compounds $[MZn_4Cl_4(L)_6]$ (M^{II} = Zn, Fe, Co, Ni, or Cu; L = 5,6-dimethyl-1,2,3-benzotriazolate) were prepared containing μ_3-bridging N-donor ligands (1,2,3-benzotriazolate), which are structurally related to the fundamental secondary building unit of *M*etal−organic *F*ramework *U*lm University-4 (**MFU-4**). The unique topology of these T_d-symmetrical compounds is characterized by the nonplanar $K_{3,3}$ graph, introduced into graph theory by the mathematician Casimir Kuratowski in 1930. The following "Kuratowski-type" compounds were investigated by single-crystal X-ray structure analysis: $[MZn_4Cl_4(Me_2bta)_6]\cdot 2DMF$ (M^{II} = Zn, Fe, Co, and Cu; DMF = *N*,*N*′-dimethylformamide) and $[MZn_4Cl_4(Me_2bta)_6]\cdot 2C_6H_5Br$ (M^{II} = Co and Ni; C_6H_5Br = bromobenzene). The μ_3-bridging benzotriazolate ligands span the edges of an imaginary tetrahedron, in the center of which a redox-active octahedrally coordinated M^{II} ion is placed. Four Zn^{II} ions are located at the corners of the coordination units. Each Zn center is bound to a monodentate Cl^- anion and three N-donor atoms stemming from different benzotriazolate ligands. The fact that open-shell redox-active M^{II} ions can be introduced selectively into the central octahedral coordination sites is unambiguously proven by a combination of magnetic measurements, UV−vis spectroscopy, and energy-dispersive X-ray and inductively coupled plasma atomic emission spectrometry analysis. The phase purity of all compounds was checked by powder X-ray diffractometry, IR spectroscopy, and elemental analysis. The electronic spectra and magnetic properties of the compounds are in complete agreement with their structures determined from single-crystal data. Thermogravimetric analysis shows that all compounds possess a high thermal stability up to 673 K. The pentanuclear compounds retain their structural integrity in solution, as evidenced by time-of-flight mass spectrometry analysis and comparative solution and solid-state diffuse-reflectance spectroscopy. High stability paired with the presence of redox-active metal ions and Lewis-acidic Zn centers renders Kuratowski-type compounds structural and functional models for future **MFU-4**-type bi- and multifunctional heterogeneous catalysts.

Introduction

A rational approach toward catalytically active metal−organic frameworks (MOFs) rests on the systematic design of discrete secondary building units (SBUs)[1] that can be linked into 3D porous solids. However, while for most MOFs there is a lack of experimental evidence in favor of framework buildup from SBUs during synthesis, it seems indisputable that the availability of discrete coordination compounds comprising structures and functions similar to or identical with SBUs, into which a MOF can be formally subdivided, would represent an enormous speed-up for an efficient and rapid prototyping of functional MOFs. Discrete coordination compounds are frequently much easier to prepare in pure form, and their good solubility in common solvents allows for the investigation of their functional properties by a range of different spectroscopic techniques that are commonly available.

As a part of our ongoing research on catalytically active MOFs, we have recently started to develop thermally and solvolytically stable model coordination compounds to gain mechanistic insights into the catalytic and molecular-sieving

*To whom correspondence should be addressed. E-mail: dirk.volkmer@uni-ulm.de. Tel: (+)49 (0)731 50-23921. Fax: (+)49 (0)731 50-23039.

(1) (a) Eddaoudi, M.; Moler, D. B.; Li, H.; Chen, B.; Reineke, T. M.; O'Keeffe, M.; Yaghi, O. M. *Acc. Chem. Res.* **2001**, *34*, 319. (b) Yaghi, O. M.; O'Keeffe, M.; Ockwig, N. W.; Chae, H. K.; Eddaoudi, M.; Kim, J. *Nature* **2003**, *423*, 705. (c) Tranchemontagne, D. J.; Mendoza-Cortés, J. L.; O'Keeffe, M.; Yaghi, O. M. *Coord. Chem. Rev.* **2008**, *38*, 1257.

 Published on Web 07/16/2010

properties exhibited by our recently synthesized **MFU-1**,[2] **MFU-3**,[3] and **MFU-4**[4] types of porous frameworks. An intensive literature survey for coordination compounds, which are structurally related to the SBUs from which **MFU-4** could be formally erected, revealed the existence of a class of coordination compounds with the chemical formula $[M_5(L)_4(OH)_x(L')_{6-x}]$ (M^{II} = first-row transition-metal ion; L = β-diketonate or nitrate; L′ = 1,2,3-triazolate; x = 0 and 1).[5] However, the peripheral M^{II} ions in these compounds are either penta- or hexacoordinated with bidentate β-diketonate, nitrate, and/or monodentate solvent molecules and are thus structurally related, though not strictly isotypic, to **MFU-4**-type SBUs. In order to achieve a better structural congruence with **MFU-4**, we have thus developed a novel family of coordination compounds, represented by the chemical formula $[M^{II}Zn_4Cl_4(L)_6]$, in which the peripheral Zn ions are tetrahedrally coordinated (Figure 1). These compounds should best serve the purpose of **MFU-4** model compounds that could be screened for catalytic activities in homogeneous test reactions. By this approach, we hope to gain further insights into catalytic and functional properties, which then might be transferable to the design of future **MFU-4**-type heterogeneous catalysts.

Tri- or tetranuclear oxo-bridged basic metal carboxylates have been known for decades and serve as discrete low-molecular counterparts for most of the MOFs containing polydentate arylcarboxylates as linkers. A huge variety of homo- and heterotrinuclear carboxylates[6] $[M_3O(L)_6]^{n+}$ (M^{III} = transition metal ion; L = bridging carboxylate)

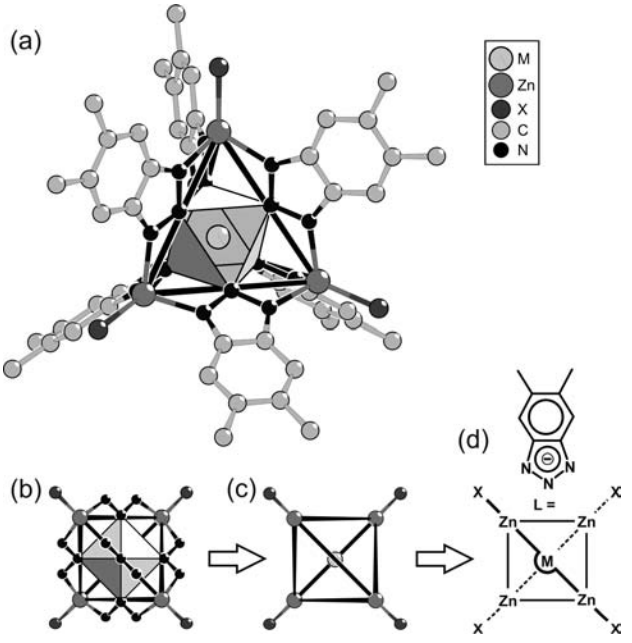

Figure 1. (a) Ball-and-stick representation of $[M^{II}Zn_4X_4(L)_6]$ " Kuratowski-type" coordination units, highlighting the central octahedral coordination site that results from six N-donor atoms situated at the centers of the edges of an imaginary tetrahedron, which is spanned by the four Zn^{II} ions at the corners. (b) Simplified representation of metal centers and ligand donor atoms. (c and d) Derivation (cf. the discussion on the graph theoretical representation) of a rational graphical scheme representing the connectivity of the coordination units.

show moderate stability against hydro/solvolysis and provide examples of low-molecular-weight analogues of many isoreticular frameworks within the **MIL** series[7] and **POST-1**.[8] Several basic zinc[9] or beryllium[10] carboxylates $[M_4O(L)_6]$ are structurally related to the coordination units of prototypic **MOF-5**[11] and its topologically related[1,12] porous frameworks. However, these compounds are hydro/solvolytically unstable[9c,d] and hence will pose difficulties when their activity in homogeneous test reactions is investigated. Relating to our recent work, all attempts to prepare model compounds of the SBU found in **MFU-1** (which is topologically related to **MOF-5**) have failed in our hands, although single-crystal structural data of the compound $[Co_4^{II}O(dmpz)_6]$ (dmpz = 3,5-dimethylpyrazolate) have been previously reported.[13]

(2) Tonigold, M.; Lu, Y.; Brodenkötter, B.; Rieger, B.; Bahnmüller, S.; Hitzbleck, J.; Langstein, G.; Volkmer, D. *Angew. Chem., Int. Ed.* **2009**, *48*, 7546.

(3) Lu, Y.; Tonigold, M.; Brodenkötter, B.; Volkmer, D.; Hitzbleck, J.; Langstein, G. *Z. Anorg. Allg. Chem.* **2008**, *634*, 2411.

(4) Biswas, S.; Grzywa, M.; Nayek, H. P.; Dehnen, S.; Senkovska, S.; Kaskel, S.; Volkmer, D. *Dalton Trans.* **2009**, 6487.

(5) (a) Marshall, J. H. *Inorg. Chem.* **1978**, *17*, 3711. (b) Himes, V. L.; Mighell, A. D.; Siedle, A. R. *J. Am. Chem. Soc.* **1981**, *103*, 211. (c) Kokoszka, G. F.; Baranowski, J.; Goldstein, C.; Orsini, J.; Mighell, A. D.; Himes, V. L.; Siedle, A. R. *J. Am. Chem. Soc.* **1983**, *105*, 5627. (d) Handley, J.; Collison, D.; Garner, C. D.; Helliwell, M.; Docherty, R.; Lawson, J. R.; Tasker, P. A. *Angew. Chem., Int. Ed. Engl.* **1993**, *32*, 1036. (e) Bakalbassis, E. G.; Diamantopoulou, E.; Perlepes, S. P.; Raptopoulou, C. P.; Tangoulis, V.; Terzis, A.; Zafiropoulos, T. F. *J. Chem. Soc., Chem. Commun.* **1995**, 1347. (f) Tangoulis, V.; Raptopoulou, C. P.; Terzis, A.; Bakalbassis, E. G.; Diamantopoulou, E.; Perlepes, S. P. *Inorg. Chem.* **1998**, *37*, 3142. (g) Murrie, M.; Collison, D.; Garner, C. D.; Helliwell, M.; Tasker, P. A.; Turner, S. S. *Polyhedron* **1998**, *17*, 3031. (h) Tangoulis, V.; Raptopoulou, C. P.; Terzis, A.; Bakalbassis, E. G.; Diamantopoulou, E.; Perlepes, S. P. *Mol. Cryst. Liq. Cryst.* **1999**, *335*, 463. (i) Jinling, W.; Ming, Y.; Yun, Y.; Shuming, Z.; Fangming, M. *Chin. Sci. Bull.* **2002**, *47*, 890. (j) Yuan, Y.-X.; Wei, P.-J.; Qin, W.; Zhang, Y.; Yao, J.-L.; Gu, R.-A. *Eur. J. Inorg. Chem.* **2007**, 4980. (k) Biswas, S.; Tonigold, M.; Volkmer, D. *Z. Anorg. Allg. Chem.* **2008**, *634*, 2532. (l) Bai, Y.-L.; Tao, J.; Huang, R. B.; Zheng, L. S. *Angew. Chem., Int. Ed.* **2008**, *47*, 5344. (m) Wang, X. L.; Qin, C.; Wu, S.-X.; Shao, K.-Z.; Lan, Y. Q.; Wang, S.; Zhu, D. S.; Su, Z.-M.; Wang, E.-B. *Angew. Chem., Int. Ed.* **2009**, *48*, 5291. (n) Gkioni, C.; Psycharis, V.; Raptopoulou, C. P. *Polyhedron* **2009**, *28*, 3425.

(6) (a) Hathaway, B. J. In *Comprehensive Coordination Chemistry*; Wilkinson, G., Ed.; Pergamon: Oxford, U.K., 1987; Vol. *2*. (b) Cannon, R. D.; White, R. P. *Prog. Inorg. Chem.* **1988**, *36*, 195.

(7) (a) Serre, C.; Millange, F.; Surblé, S.; Férey, G. *Angew. Chem., Int. Ed.* **2004**, *43*, 6285. (b) Férey, G.; Serre, C.; Mellot-Draznieks, C.; Millange, F.; Surblé, S.; Dutour, J.; Margiolaki, I. *Angew. Chem., Int. Ed.* **2004**, *43*, 6296. (c) Mellot-Draznieks, C.; Serre, C.; Surblé, S.; Audebrand, N.; Férey, G. *J. Am. Chem. Soc.* **2005**, *127*, 16273. (d) Férey, G.; Mellot-Draznieks, C.; Serre, C.; Millange, F.; Dutour, J.; Surblé, S.; Margiolaki, I. *Science* **2005**, *309*, 2040. (e) Surblé, S.; Serre, C.; Mellot-Draznieks, C.; Millange, F.; Férey, G. *Chem. Commun.* **2006**, 284. (f) Surblé, S.; Millange, F.; Serre, C.; Düren, T.; Latroche, M.; Bourrelly, S.; Llewellyn, P. L.; Férey, G. *J. Am. Chem. Soc.* **2006**, *128*, 14889. (g) Horcajada, P.; Surblé, S.; Serre, C.; Hong, D.-Y.; Seo, Y.-K.; Chang, J.-S.; Grenèche, J.-M.; Margiolaki, I.; Férey, G. *Chem. Commun.* **2007**, 2820.

(8) Seo, J. S.; Whang, D.; Lee, H.; Jun, S. I.; Oh, J.; Jeon, Y. J.; Kim, K. *Nature* **2000**, *404*, 982.

(9) (a) Kyoama, H.; Saito, Y. *Bull. Chem. Soc. Jpn.* **1954**, *27*, 112. (b) Gordon, R. M.; Silver, H. B. *Can. J. Chem.* **1983**, *61*, 1218. (c) Clegg, W.; Harbron, D. R.; Homan, C. D.; Hunt, P. A.; Little, I. R.; Straughan, B. P. *Inorg. Chim. Acta* **1991**, *186*, 51. (d) Amico, D. B. D.; Cadderazzo, F.; Labella, L.; Marchetti, F.; Pampaloni, G. *Inorg. Chem. Commun.* **2002**, *5*, 733. (e) McCowan, C. S.; Groy, T. L.; Caudle, M. T. *Inorg. Chem.* **2002**, *41*, 1120. (f) Hou, H.; Li, L.; Li, G.; Fan, Y.; Zhu, Y. *Inorg. Chem.* **2003**, *42*, 3501. (g) Karmakar, A.; Baruah, J. B. *Polyhedron* **2008**, *27*, 3409.

(10) (a) Pauling, L.; Sherman, J. *Proc. Natl. Acad. Sci. U.S.A.* **1934**, *20*, 340. (b) Tulinsky, A.; Worthington, C. R.; Pignataro, E. *Acta Crystallogr.* **1959**, *12*, 623. (c) Tulinsky, A.; Worthington, C. R. *Acta Crystallogr.* **1959**, *12*, 626. (d) Tulinsky, A. *Acta Crystallogr.* **1959**, *12*, 634.

(11) Li, H.; Eddaoudi, M.; O'Keeffe, M.; Yaghi, O. M. *Nature* **1999**, *402*, 276.

(12) (a) Yaghi, O. M.; Li, H.; Davis, C.; Richardson, D.; Groy, T. L. *Acc. Chem. Res.* **1998**, *31*, 474. (b) Rosi, N. L.; Eddaoudi, M.; Kim, J.; O'Keeffe, M.; Yaghi, O. M. *CrystEngComm* **2002**, *4*, 401. (c) Rowsell, J. L. C.; Yaghi, O. M. *Microporous Mesoporous Mater.* **2004**, *73*, 3.

(13) Ehlert, M. K.; Rettig, S. J.; Storr, A.; Thompson, R. C.; Trotter, J. *Acta Crystallogr.* **1994**, *C50*, 1023.

In contrast to the former compound, the synthesis of suitable model compounds relating to **MFU-4** proved to be straightforward. In the following study, syntheses and comparative magnetostructural and spectroscopic investigations on homo- and heteropentanuclear coordination compounds $[M^{II}Zn_4Cl_4(L)_6]$ (M^{II} = Zn, Fe, Co, Ni, or Cu; L = 5,6-dimethyl-1,2,3-benzotriazolate) are presented, for which we would like to propose the term "Kuratowski-type" coordination units.

From a topological point of view, the coordination units $[MZn_4Cl_4(L)_6]$ represent the rare class of minimum nonplanar building units having T_d point group symmetry and $K_{3,3}$ as a molecular graph (Figure 1; see also Figure 14), constituting versatile models of a future library of structurally related cubic **MFU-4**-type porous frameworks. As shown in Figure 1, the homopentanuclear $[Zn_5Cl_4(L)_6]$ coordination unit has two different coordination sites: one central octahedral site and four tetrahedral sites at peripheral positions. Substituting the central octahedrally coordinated Zn^{II} ion with an open-shell d transition-metal ion M^{II} causes a huge gain in the crystal-field stabilization energy. Therefore, the use of stoichiometric mixtures of different metal salts (M^{II}/Zn^{II}) enabled us to synthesize a series of heteropentanuclear compounds in which the open-shell M^{II} ions occupy the octahedral coordination sites. To the best of our knowledge, these are the first examples of heterometallic compounds containing 1,2,3-triazolates. The open-shell M^{II} ions might act as redox catalysts in homogeneous reactions. Moreover, the coordinatively unsaturated Zn^{II} ions may fill up (either permanently or transiently) the number of coordinated ligands[5a,d−i,k−n] and may thus be employed as Lewis acid catalysts for a wide variety of homogeneous reactions (e.g., Diels−Alder, Aldol, Mannich, Friedel−Crafts, 1,2 and 1,4 addition, oxidation and reduction, esterification, and Claisen rearrangement).[14] Here emphasis will be laid upon syntheses and magnetostructural investigations, while reports on selected functional properties of the title compounds will follow in due course.

Experimental Section

Materials and General Methods. All starting materials were of reagent grade and were used as received from the commercial supplier. Fourier transform infrared (FT-IR) spectra were recorded from KBr pellets in the range 4000−400 cm^{-1} on a Bruker IFS FT-IR spectrometer. The following indications are used to characterize absorption bands: very strong (vs), strong (s), medium (m), weak (w), shoulder (sh), and broad (br). UV−vis diffuse-reflectance spectroscopy (DRS) spectra were recorded on an Analytik Jena Specord 50 UV−vis spectrometer in the range of 300−1100 nm and converted into normal absorption spectra with the Kubelka−Munk function.[15] The lamps change at 320 nm, and the mirrors change at 370, 400, 700, and 900 nm. UV−vis solution spectra were measured using the same UV−vis spectrometer. Elemental analyses (C, H, and N) were carried out on a Perkin-Elmer 2400 elemental analyzer. Thermogravimetric analysis (TGA) was performed with a TGA/SDTA851 Mettler Toledo analyzer in a temperature range of 298−1373 K in flowing nitrogen at a heating rate of 10 K min^{-1}. Ambient-temperature powder X-ray diffraction (PXRD) patterns were measured using a Philips X'Pert PRO powder diffractometer operated at 40 kV and 40 mA for Cu radiation (λ = 1.5406 Å) with a scan speed of 30 s $step^{-1}$ and a step size of 0.008°. The simulated powder patterns were calculated using single-crystal X-ray diffraction data. Energy-dispersive X-ray (EDX) analyses were performed on an EDAX (Phönix) X-ray detection system with a 30 mm^2 SUTW window. Inductively coupled plasma atomic emission spectrometry analysis (ICP-AES) analyses were carried out with a Thermo Scientific iCap 6500 emission spectrometer. Time-of-flight mass spectrometry (TOF-MS) analyses were performed with a Jeol JMS-T100GCV time-of-flight mass spectrometer and a liquid injection field desorption ionization source. Magnetic susceptibility data of **2a**, **3a**, **4b**, and **5a** were determined using a SQUID magnetometer (Quantum Design MPMS-XL5) in the temperature range T = 2.0−290 K and at an applied field of B_0 = 0.1−5.0 T. Susceptibility data were corrected for sample holder [poly(tetrafluoroethylene) capsules] and diamagnetic contributions. The latter was determined from measurement of the diamagnetic compound **1a** and used as the uniform value $\chi_{dia} = 0.981 \times 10^{-8}$ m^3 mol^{-1} for **2a**, **3a**, **4b**, and **5a**.

Safety Note! *Perchlorate salts and benzotriazolate complexes are potentially explosive, and caution should be exercised when dealing with such materials*. However, the small quantities used in this study were not found to present a hazard.

The syntheses, crystal structures, and analytical and spectroscopic data of compounds $[Zn_5Cl_4(Me_2bta)_6]\cdot 2DMF$ (**1a**) and $[CoZn_4Cl_4(Me_2bta)_6]\cdot 2DMF$ (**3a**), where DMF = *N*,*N*′-dimethylformamide, were previously reported by the Volkmer group.[5k] Elemental analyses and the frequencies of IR bands for all of the compounds are presented in Tables S1 and S2 (Supporting Information), respectively.

Synthesis of $[Zn_5Cl_4(Me_2bta)_6]\cdot 2C_6H_5Br$ (1b). A solution of lutidine (1.05 mL, 9.04 mmol) in methanol (5 mL) was added to a solution of Me_2btaH (1.50 g, 9.08 mmol) in the same solvent (20 mL). To this mixture was added a methanol solution (10 mL) of $ZnCl_2$ (1.03 g, 7.55 mmol). The mixture was stirred at room temperature for 30 min, and the resulting white solid (1.84 g) was collected by filtration, washed with 10 mL of MeOH, and air-dried. This solid was dissolved in hot bromobenzene (35 mL), and the resulting clear solution was allowed to cool to room temperature, leading to clear octahedrally shaped crystals of **1b**. The yield was 1.68 g (1.01 mmol, 67%).

Syntheses of $[MZn_4Cl_4(Me_2bta)_6]\cdot 2DMF$ [M^{II} = Fe (2a), Cu (5a)]. Both compounds were prepared identically in a manner as described in ref 5k.

$[FeZn_4Cl_4(Me_2bta)_6]\cdot 2DMF$ (2a). A mixture of $Fe(ClO_4)_2\cdot 6H_2O$ (37 mg, 0.14 mmol), anhydrous $ZnCl_2$ (80 mg, 0.59 mmol), and Me_2btaH (146 mg, 0.88 mmol) was placed in a small vial and dissolved in 3 mL of DMF. The vial was placed in a larger vial (30 mL) containing 6 mL of DMF and 205 μL of 2,6-lutidine. The larger vial was sealed and left undisturbed for 4 days. The resulting yellow octahedral crystals were collected by filtration, washed three times with 1 mL of DMF, and air-dried to yield 75 mg of **2a** (0.05 mmol, 36%).

$[CuZn_4Cl_4(Me_2bta)_6]\cdot 2DMF$ (5a). This compound was obtained, after 2 weeks, as brown octahedral crystals by the procedure described for **2a**, with the exception of the addition of $Cu(NO_3)_2\cdot 3H_2O$ (35 mg, 0.14 mmol) instead of $Fe(ClO_4)_2\cdot 6H_2O$. Yield: 80 mg (0.053 mmol, 39%).

Syntheses of $[MZn_4Cl_4(Me_2bta)_6]\cdot 2C_6H_5Br$ [M^{II} = Fe (2b), Co (3b), Ni (4b), Cu (5b)]. All of these compounds were prepared in an analogous manner as described for **1b** except that the $ZnCl_2$:metal nitrate/perchlorate ratio used was 1:4.

$[FeZn_4Cl_4(Me_2bta)_6]\cdot 2C_6H_5Br$ (2b). Yellow octahedral crystals of **2b** were obtained by the procedure described for **1b**, with the exception of the addition of a mixture of $ZnCl_2$ (0.82 g, 6.01 mmol) and $Fe(ClO_4)_2\cdot 6H_2O$ (0.38 g, 1.50 mmol) instead of $ZnCl_2$. Yield: 1.71 g (1.03 mmol, 69%).

$[CoZn_4Cl_4(Me_2bta)_6]\cdot 2C_6H_5Br$ (3b). Light-green octahedral crystals of **3b** were obtained by the procedure described for **2b**, with

(14) *Acid Catalysis in Modern Organic Syntheses*; Yamamoto, H., Ishihara, K., Eds.; Wiley-VCH: Weinheim, Germany, 2008; Vol. *1*, pp 151−174.

(15) Wendlandt, W. W.; Hecht, H. G. *Reflectance Spectroscopy*; Interscience Publishers/JohnWiley & Sons: New York, 1966.

Table 1. Single-Crystal Data and Refinement Summary for **2a**, **3b**, **4b**, and **5a**

	2a	**3b**	**4b**	**5a**
formula	$C_{48}H_{48}Cl_4FeN_{18}Zn_4$	$C_{60}H_{58}Br_2Cl_4CoN_{18}Zn_4$	$C_{60}H_{58}Br_2Cl_4N_{18}NiZn_4$	$C_{48}H_{48}Cl_4CuN_{18}Zn_4$
fw	1336.18	1653.27	1653.05	1343.86
T/K	293(2)	293(2)	296(2)	293(2)
λ/Å	0.710 73	0.710 73	0.710 73	0.710 73
cryst dimens/mm	0.31 × 0.31 × 0.39	0.24 × 0.24 × 0.32	0.36 × 0.36 × 0.24	0.27 × 0.31 × 0.33
cryst syst	cubic	cubic	cubic	cubic
space group	$Fd\bar{3}m$	$Fd\bar{3}m$	$Fd\bar{3}m$	$Fd\bar{3}m$
a/Å	23.456(3)	23.737(3)	23.7160(4)	23.421(3)
V/Å^3	12905(3)	13375(3)	13339.0(4)	12848(3)
Z	8	8	8	8
D_c/g cm^{-3}	1.375	1.642	1.646	1.389
M/mm^{-1}	1.895	3.065	3.107	2.009
F(000)	5408	6632	6640	5432
θ range/deg	2.46−25.96	2.43−25.91	2.43−32.35	2.46−25.87
measd reflns	24 622	24 077	54 846	24 421
indep reflns	648	673	1182	646
data/restraints/param	648/0/43	673/0/55	1182/0/55	646/0/44
R1 [$I > 2\sigma(I)$][a]	0.0653	0.0316	0.0362	0.0779
wR2 (all data) [b]	0.2239	0.0849	0.0994	0.2193
GOF on F^2	1.278	1.085	1.172	1.049
$\Delta\rho_{max,min}$/e Å^{-3}	2.919, −0.430	1.004, −0.268	0.595, −0.453	2.625, −0.419

[a] $R1 = \sum||F_o| - |F_c||/\sum|F_o|$. [b] $wR2 = \{\sum[w(F_o^2 - F_c^2)^2]/\sum[w(F_o^2)^2]\}^{1/2}$.

Scheme 1[a]

Homopentanuclear compounds $[Zn_5Cl_4(Me_2bta)_6]$:

$$5\ ZnCl_2 + 6\ Me_2btaH + 6\ B \xrightarrow[RT]{solvent} [Zn_5Cl_4(Me_2bta)_6] + 6\ \overset{\oplus}{B}H + 6\ \overset{\ominus}{Cl}$$

Heteropentanuclear compounds $[MZn_4Cl_4(Me_2bta)_6]$:

$$MX_2(H_2O)_6 + 4\ ZnCl_2 + 6\ Me_2btaH + 6\ B \xrightarrow[RT]{solvent} [MZn_4Cl_4(Me_2bta)_6] + 6\ \overset{\oplus}{B}H + 4\ \overset{\ominus}{Cl} + 2\ \overset{\ominus}{X} + 6\ H_2O$$

[a] Chemical equations for the preparation of all of the compounds demonstrated in this work. B = 2,6-lutidine; M^{II} = Zn, Fe, Co, Ni, Cu; X = NO_3 for **3a**, **3b**, **5a**, and **5b** and ClO_4 for **2a**, **2b**, and **4b**; solvent = DMF for **1a**, **2a**, **3a**, and **5a** and methanol for **1**−**5b**.

the exception of the addition of $Co(NO_3)_2 \cdot 6H_2O$ (0.44 g, 1.50 mmol) instead of $Fe(ClO_4)_2 \cdot 6H_2O$. Yield: 1.22 g (0.74 mmol, 49%).

$[NiZn_4Cl_4(Me_2bta)_6] \cdot 2C_6H_5Br$ (4b). Light-blue octahedral crystals of **4b** were obtained by the procedure described for **2b**, with the exception of the addition of $Ni(ClO_4)_2 \cdot 6H_2O$ (0.55 g, 1.50 mmol) instead of $Fe(ClO_4)_2 \cdot 6H_2O$. Yield: 1.06 g (0.64 mmol, 43%).

$[CuZn_4Cl_4(Me_2bta)_6] \cdot 2C_6H_5Br$ (5b). Brown octahedral crystals of **5b** were obtained by the procedure described for **2b**, with the exception of the addition of $Cu(NO_3)_2 \cdot 3H_2O$ (0.37 g, 1.50 mmol) instead of $Fe(ClO_4)_2 \cdot 6H_2O$. Yield: 1.75 g (1.05 mmol, 70%).

Structure Determination. Solid-state structures of **1a**, **2a**, **3a**, **3b**, **4b**, and **5a** were determined from single-crystal X-ray diffraction data. The intensity data of **4b** were collected with a Bruker APEXII CCD diffractometer employing monochromated Mo Kα radiation (λ = 0.710 73 Å) at T = 296 K. For all other compounds, the data were recorded on a STOE IPDS diffractometer using Mo Kα radiation with graphite monochromatization (λ = 0.710 73 Å) at T = 293 K. The initial structures of all compounds were solved by direct methods and refined by full-matrix least-squares techniques based on F^2 using the *SHELXL-97* program.[16] Details of single-crystal data collection and refinement of **2a**, **3b**, **4b**, and **5a** are summarized in Table 1.

Results and Discussion

Syntheses. All metal compounds described here are crystalline and stable in air at ambient conditions. All compounds are sparingly soluble in solvents such as chlorobenzene, 1,2-dichlorobenzene, 1,3-dichlorobenzene, 1,2,4-trichlorobenzene, bromobenzene, xylene, mesitylene, *N*,*N*′-dimethylacetamide (DMA), 1-methyl-2-pyrrolidone, or ethyl acetate.

Compounds **1a**, **2a**, **3a**, and **5a** were crystallized from a DMF solution containing suitable metal precursors and a ligand with a calculated stoichiometric ratio employing slow vapor diffusion of lutidine into the crystallization vial. However, this strategy was unsuccessful for the preparation of heteropentanuclear compound $[NiZn_4Cl_4(Me_2bta)_6] \cdot 2DMF$ (**4a**). Therefore, an alternate synthetic strategy, namely, the dropwise addition of lutidine, was applied for the synthesis of this compound. In fact, the direct addition of lutidine to a methanol solution containing stoichiometric amounts of the metal salts and ligand, followed by recrystallization of the quickly precipitated solid from bromobenzene, produced light-blue octahedral crystals of **4b**. During the course of our investigations, it was also found that a series of homo- and heteropentanuclear coordination compounds of the general formula $[MZn_4Cl_4(Me_2bta)_6] \cdot 2C_6H_5Br$ [M^{II} = Zn (**1b**), Fe (**2b**), Co (**3b**), Ni (**4b**), Cu (**5b**)] can likewise be synthesized in large quantities from a methanol solution employing the "direct addition of lutidine" approach, which is much faster than the "vapor diffusion of lutidine" route. All preparations are summarized in Scheme 1.

Characterization. The phase purity of all metal compounds was confirmed by elemental analysis and PXRD.

(16) Sheldrick, G. M. *Acta Crystallogr.* **2008**, *A64*, 112.

The experimental PXRD patterns are consistent with the simulated ones, as determined from the single-crystal X-ray diffraction data (Figures S1−S4, Supporting Information). All compounds in each set of derivatives (each set having either DMF or brombenzene as occluded solvent molecules) possess similar PXRD patterns (Figure S5, Supporting Information). Slight differences in intensities and peak positions between the PXRD patterns of the two sets of compounds are due to the solvent molecules.

The FT-IR spectra of all of the compounds (Figures S6 and S7, Supporting Information) show characteristic strong bands of the coordinated Me_2btaH ligand at ca. 1000 and 1200 cm^{-1}, which are assigned to C−H out-of-plane bending vibrations and vibrations involving both triazole ring breathing and C−H in-plane bending, respectively.[17] The IR spectra of all isostructural metal compounds are very similar, as expected. The occluded solvent molecules cause slight differences between the IR spectra of both sets of compounds. The strong absorption band at ca. 1680 cm^{-1} in the case of **1a**, **2a**, **3a**, and **5a** is due to the C=O stretching frequency of noncoordinated DMF molecules. The intense IR absorbance at ca. 750 cm^{-1} for **1**−**5b** is attributed to occluded bromobenzene molecules.[18]

In order to examine the thermal stability of the compounds, TGA was performed on crystalline samples of all compounds in a nitrogen atmosphere. All compounds show high thermal stability up to 673 K. In the TGA curve of **2a** (Figure S8, Supporting Information), the first mass loss of 11.5% in the temperature range 433−643 K is attributed to the removal of two noncoordinated DMF molecules per formula unit (calcd: 9.9%). In the TGA curve of **5a** (Figure S9, Supporting Information), the first mass loss is 8.5% from 418 to 573 K and the second step is 2.8% from 573 to 643 K, both assigned to the liberation of two noncoordinated DMF molecules per formula unit (calcd: 9.8%). In the TGA curves of **1**−**5b** (Figure S10, Supporting Information), the first mass loss steps (17.6%, **1b**; 17.0%, **2b**; 17.9%, **3b**; 20.1%, **4b**; 17.8%, **5b**) in the temperature range 423−673 K are attributed to the removal of two occluded bromobenzene molecules per formula unit (calcd: 18.9%, **1b**; 19.0%, **2b**; 19.0%, **3b**; 19.0%, **4b**; 18.9%, **5b**). For all of the compounds, any mass loss step that occurs at a temperature above 673 K can be assigned to decomposition of the compounds.

EDX measurements (Figures S11−S17, Supporting Information) performed on crystalline samples show the following M (M = Fe, Co, Ni, or Cu)/Zn ratios: Fe/Zn = 3.8, **2a**; Cu/Zn = 3.79, **5a**; Fe/Zn = 3.87, **2b**; Co/Zn = 3.76, **3b**; Ni/Zn = 4.0, **4b**; Cu/Zn = 3.99, **5b**. The determined ratios closely match the theoretical M/Zn ratio of 1:4.0, thus confirming the presence of open-shell metal atoms M in all heteropentanuclear compounds.

ICP-AES analyses were carried out on **2a**, **3a**, **3b**, **4b**, and **5a** in order to derive more precise M/Zn ratios. The experimental weight percentages of the metal ions (Table S3, Supporting Information) are in agreement with the estimated ones, which unequivocally prove the coexistence of open-shell M and Zn ions in the expected ratios.

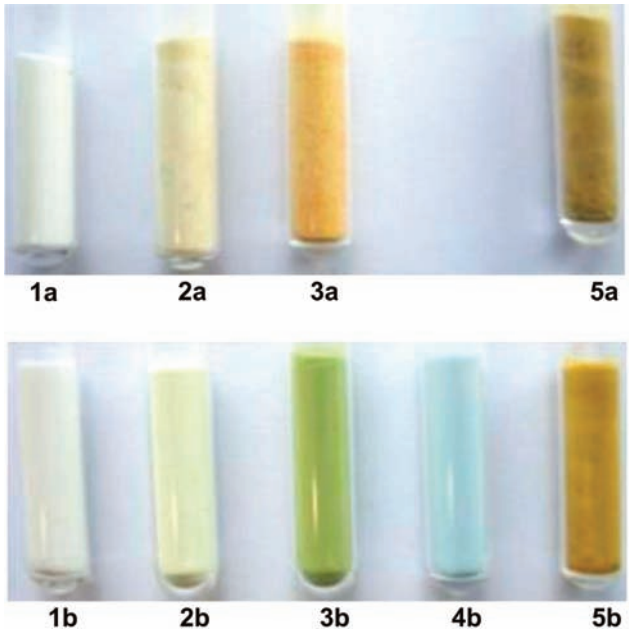

Figure 2. Photographs of Kuratowski-type compounds prepared by different methods as described in Scheme 1. Top row: set of compounds recrystallized from DMF. Bottom row: set of compounds recrystallized from bromobenzene. Compound index: $[M^{II}Zn_4Cl_4(Me_2bta)_6]\cdot 2DMF$ with M^{II} = Zn (**1a**), Fe (**2a**), Co (**3a**), Cu (**5a**); $[M^{II}Zn_4Cl_4(Me_2bta)_6]\cdot 2C_6H_5Br$ with M^{II} = Zn (**1b**), Fe (**2b**), Co (**3b**), Ni (**4b**), Cu (**5b**).

In order to ensure the structural integrity of the pentanuclear compounds in solution, TOF-MS analyses were performed with ethyl acetate solutions of **1a** and **5a** (Figures S18 and S19, Supporting Information). The m/z ratios (1345.7, **1a**; 1343.9, **5a**) calculated for the desolvated compounds are in agreement with the observed m/z ratios (1345.9, **1a**; 1344.2, **5a**). Moreover, the simulated and experimental isotopic patterns of the two compounds are quite similar. These results confirm that the compounds maintain their structural integrity in solution. Notably, the stability of a structurally related homopentanuclear Zn^{II} compound in a DMA solution at 358 K has been previously verified by electrospray ionization mass spectrometry studies.[5m]

UV−Vis Spectroscopy. The UV−vis spectra of **2a**, **2b**, **3a**, **3b**, **4b**,**5a**, and **5b** in solution display a common absorption band in the UV region at around 380 nm, which corresponds to the intraligand n→π^* transition.[19] In addition, all of these compounds exhibit well-developed bands in the range of 400−1100 nm (Figures 3a, 4a, 5a, and 6a) owing to the d−d transitions of octahedrally coordinated Fe^{II}, Co^{II}, Ni^{II}, and Cu^{II} ions.[20]

Compounds **2a** and **2b** show one broad absorption band in the region 700−1050 nm due to the spin-allowed transition $^5T_{2g} \rightarrow {}^5E_g$. The simple nature of the UV−vis spectra of these two compounds indicates that Fe^{II} ions are in a high-spin state, inducing no tetragonal distortion in the compounds.

Compounds **3a** and **3b** show three absorption bands at 900, 540, and 500 nm, which can be attributed to the

(17) Rubim, J.; Gutz, I. G. R.; Sala, O.; Orville-Thomas, W. J. *J. Mol. Struct.* **1983**, *100*, 571.

(18) Chien, Y. C.; Wang, H. P.; Lin, K. S.; Huang, Y.-J.; Yang, Y.-W. *Chemosphere* **2000**, *40*, 383.

(19) Gilbert, A.; Baggott, J. *Essentials of Molecular Photochemistry*; CRC Press: Boca Raton, FL, 1991; pp 87−89.

(20) (a) Lever, A. B. P. *Inorganic Electronic Spectroscopy*; Elsevier Publishing Company: Amsterdam, The Netherlands, 1968; Chapter 9. (b) The Dq and B values were estimated by using the transition energy ratio diagrams on pp 393−400 of the same book as that in ref 20a.

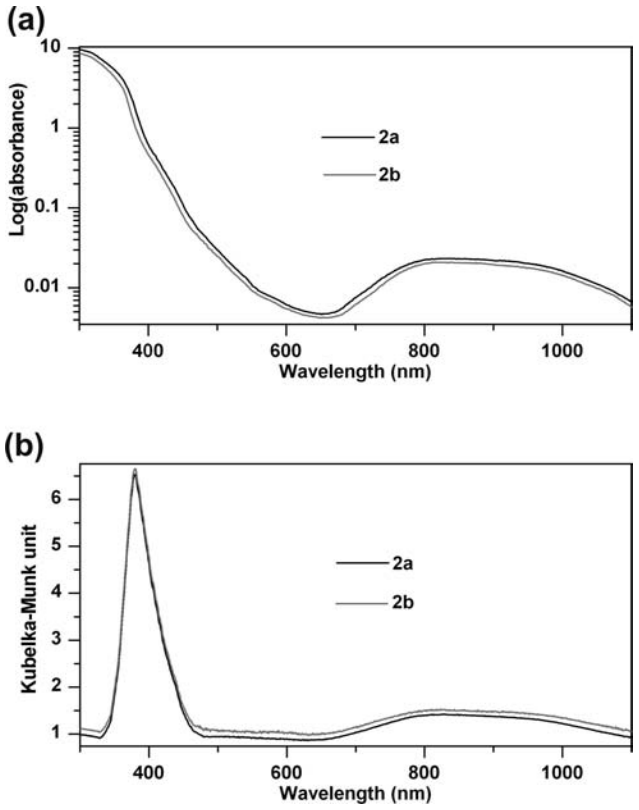

Figure 3. (a) UV−vis spectra of **2a** and **2b** in an ethyl acetate solution measured with the same concentration of 2.2×10^{-3} (M). (b) UV−vis DRS spectra of **2a** and **2b**.

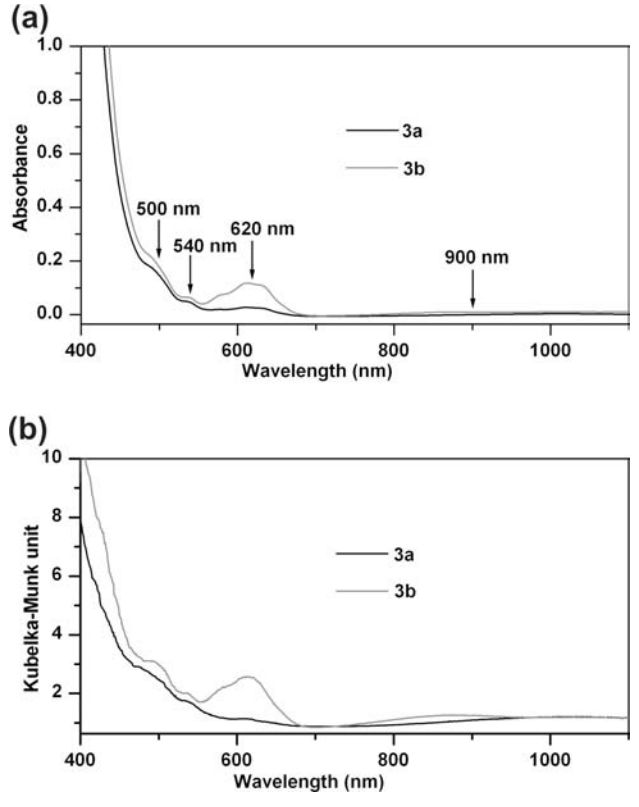

Figure 4. (a) UV−vis spectra of **3a** and **3b** in a bromobenzene solution measured with the same concentration of 2.6×10^{-3} (M). (b) UV−vis DRS spectra of **3a** and **3b**.

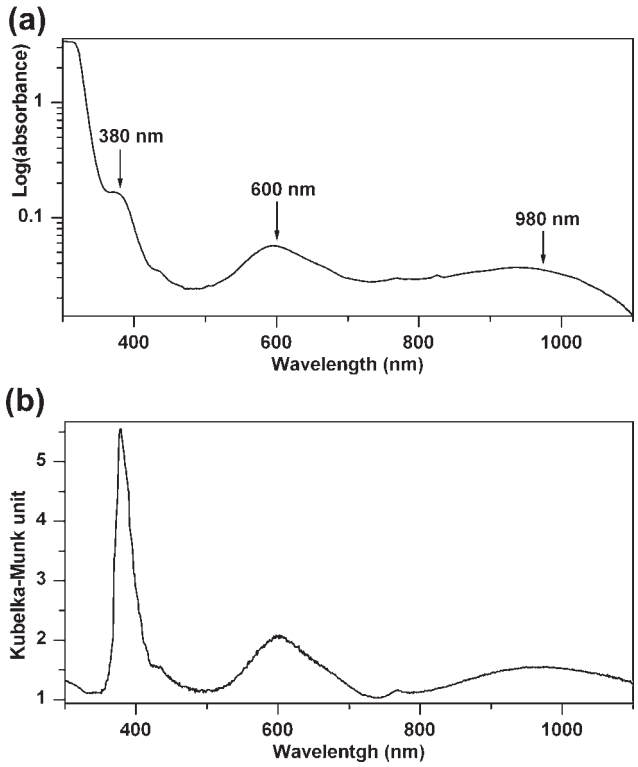

Figure 5. (a) UV−vis spectrum of **4b** in an ethyl acetate solution. (b) UV−vis DRS spectrum of **4b**.

spin-allowed transitions $^4T_{1g}(F) \rightarrow {}^4T_{2g}(F)$ (ν_1), $^4T_{1g}(P)$ (ν_2), and $^4A_{2g}$ (ν_3), respectively. The calculated values of Dq (1200 cm^{-1}) and B (665 cm^{-1}) from these transitions are comparable to those of other compounds with octahedrally coordinated Co^{II}.[20] In addition, **3b** shows a relatively stronger absorption band at 620 nm (with a shoulder at 575 nm), which is a typical position where tetrahedrally coordinated Co^{II} ions display strong absorption bands due to the spin-allowed transition $^4A_{2g} \rightarrow {}^4T_{1g}(P)$ (ν_3). This fact indicates that the fast precipitation method employed for the preparation of **3b** results in the formation of a (variable amount) of a coordination isomer of **3a**, in which some of the peripheral tetrahedrally coordinated sites are occupied by Co^{II} ions instead of Zn^{II} ions, along with the desired compound. The light-greenish **3b** (Figure 2) is therefore a mixture of the "pure" compound with orange color like **3a** and an isomeric compound showing the typical deep-blue or purple color of compounds with tetrahedrally coordinated Co^{II}.

Compound **4b** exhibits three absorption bands at 980, 600, and 380 nm due to the spin-allowed transitions $^3A_{2g} \rightarrow {}^3T_{2g}(F)$ (ν_1), $^3T_{1g}(F)$ (ν_2), and $^3T_{1g}(P)$ (ν_3), respectively. The ν_3 transition of **4b** is probably overlapped with the intraligand $n \rightarrow \pi^*$ transition. The values of Dq (1085 cm^{-1}) and B (775 cm^{-1}), which have been estimated from these transitions, are typical for compounds with octahedrally coordinated Ni^{II}.[20]

Compounds **5a** and **5b** show only one absorption band in the visible region at 700 nm, which is assigned to the spin-allowed transition $^2E_g \rightarrow {}^2T_{2g}$. The simple spectra of these types are typical for copper(II) compounds that exhibit $[CuN_6]$ octahedra without a significant Jahn−Teller distortion.

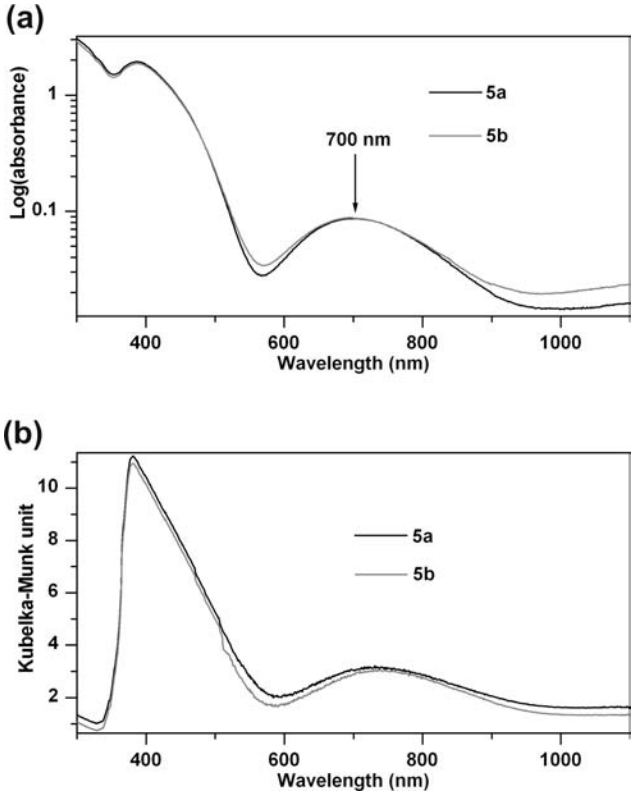

Figure 6. (a) UV−vis spectra of **5a** and **5b** in an ethyl acetate solution measured with the same concentration of 2.0×10^{-3} (M). (b) UV−vis DRS spectra of **5a** and **5b**.

The UV−vis DRS spectra of **2a**, **2b**, **3a**, **3b**, **4b**, **5a**, and **5b** (Figures 3b, 4b, 5b, and 6b) show similar absorption bands when compared to the solution UV−vis spectra, which indicates that the compounds maintain their structural integrity in solution. These electronic spectral features of the compounds are consistent with their structural and magnetic characteristics.

Structure Description. X-ray crystallographic analyses reveal that **1a**, **2a**, **3a**, **3b**, **4b**, and **5a** all crystallize in the highly symmetrical space group $Fd\bar{3}m$. The molecular structure identical with those of all pentanuclear compounds is shown in Figure 7.

Each pentanuclear coordination compound is composed of a tetrahedral arrangement of four Zn^{II} ions surrounding a fifth hexacoordinated M^{II} ion (M = Zn, Fe, Co, Ni, or Cu) in the center. The six μ_3-benzotriazolate ligands span the six edges of the (imaginary) tetrahedron. Each benzotriazolate ligand bonds to the central octahedrally coordinated metal ion through its N-donor atom in the 2 position (N^2). Six N atoms from six benzotriazolate ligands therefore complete the coordination sphere of the central metal ion, while each Zn^{II} ion is coordinated by three N atoms from three benzotriazolate ligands and one Cl atom. Notably, the atoms of **1a**, **2a**, **3a**, **3b**, **4b**, and **5a** occupy special positions within the crystal lattice, such that the asymmetric unit (Figure 8) in the cubic space group $Fd\bar{3}m$ contains only the minimum subset (=9) of atoms required for a complete representation of a pentanuclear metal complex containing six Me_2bta ligands (75 atoms for each compound, excluding H atoms). Notably, the $\eta^1{:}\eta^1{:}\eta^1{:}\mu_3$-coordination mode of benzotriazolate ligands observed in the present compounds

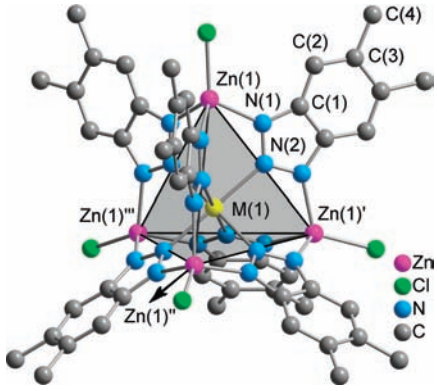

Figure 7. (a) Ball-and-stick representation of the molecular structures of **1a**, **2a**, **3a**, **3b**, **4b**, and **5a** showing the existence of an imaginary tetrahedron in each of them [M = Zn (**1a**), Fe (**2a**), Co (**3a** and **3b**), Ni (**4b**), Cu (**5a**)]. All H atoms are omitted for clarity. Symmetry operators used to create equivalent atoms are as follows: (′) $^1/_4 - x, ^1/_4 - y, z$; (″) $^1/_4 - x, y, ^5/_4 - z$; (‴) $x, ^1/_4 - y, ^5/_4 - z$. For **1a**, the labels "Zn(1)" should be replaced by "Zn(2)" to compare its bond lengths and angles with other compounds.

was previously documented for a selection of coordination compounds and coordination polymers containing Zn^{II},[4,5k,m,n,21] Co^{II},[5k,l,22] Ni^{II},[5e,f,h,l,22b] Cu^{II},[5a,d,g,i] Tl^{I},[23] and M^{III} (M = Fe, Cr, and V)[24] ions, including two mixed-valent copper[5b,c,j] compounds.

Within all homo- and heteropentanuclear metal complexes, the corresponding distances between the metal and ligating atoms are comparable.

The Zn(1)−N(1) distances for the tetrahedrally coordinated peripheral Zn atoms are in a narrow range of 2.01−2.02 Å. However, the M(1)−N(2) [M = Zn (**1a**), Fe (**2a**), Co (**3a** and **3b**), Ni (**4b**), Cu (**5a**)] distances for the octahedrally coordinated central metal (M) atoms show significantly broader variations ranging from 2.14 to 2.20 Å. Selected bond lengths are summarized in Table 2. All of these values are in agreement with literature data (1.98−2.16 Å for tetrahedrally coordinated[5k,m,n] Zn and 1.98−2.47 Å for octahedrally coordinated[5b−n] Zn, Co, Ni, or Cu) reported for structurally related metal(II) triazolate compounds. The M(1)−N(2) distances decrease with increasing atomic number [from M = Fe (**2a**) to Cu (**5a**)], a trend that is expected for high-spin transition-metal ions.

(21) Qin, Y.-Y.; Zhang, J.; Li, Z.-J.; Zhang, L.; Cao, X.-Y.; Yao, Y.-G. *Chem. Commun.* **2008**, 2532.
(22) (a) Zhang, X.-M.; Hao, Z.-M.; Zhang, W.-X.; Chen, X.-M. *Angew. Chem., Int. Ed.* **2007**, *46*, 3456. (b) Biswas, S.; Tonigold, M.; Speldrich, M.; Kögerler, P.; Volkmer, D. *Eur. J. Inorg. Chem.* **2009**, 3094.
(23) Reedijk, J.; Roelofsen, G.; Siedle, A. R.; Spek, A. L. *Inorg. Chem.* **1979**, *18*, 1947.
(24) (a) Collison, D.; McInnes, E. J. L.; Brechin, E. K. *Eur. J. Inorg. Chem.* **2006**, 2725. (b) Tabernor, J.; Jones, L. F.; Heath, S. L.; Muryn, C.; Aromí, G.; Ribas, J.; Brechin, E. K.; Collison, D. *Dalton Trans.* **2004**, 975. (c) Laye, R. H.; Wei, Q.; Mason, P. V.; Shanmugam, M.; Teat, S. J.; Brechin, E. K.; Collison, D.; McInnes, E. J. L. *J. Am. Chem. Soc.* **2006**, *128*, 9020. (d) Jones, L. F.; Brechin, E. K.; Collison, D.; Harrison, A.; Teat, S. J.; Wernsdorfer, W. *Chem. Commun.* **2002**, 2974. (e) Jones, L. F.; Rajaraman, G.; Brockman, J.; Murugesu, M.; Raftery, J.; Teat, S. J.; Wernsdorfer, W.; Christou, G.; Brechin, E. K.; Collison, D. *Chem.—Eur. J.* **2004**, *10*, 5180. (f) Jones, L. F.; Brechin, E. K.; Collison, D.; Raftery, J.; Teat, S. J. *Inorg. Chem.* **2003**, *42*, 6971. (g) Jones, L. F.; Raftery, J.; Teat, S. J.; Collison, D.; Brechin, E. K. *Polyhedron* **2005**, *24*, 2443. (h) Shaw, R.; Laye, R. H.; Jones, L. F.; Low, D. M.; Talbot-Eeckelaers, C.; Wei, Q.; Milios, C. J.; Teat, S.; Helliwell, M.; Raftery, J.; Evangelisti, M.; Affronte, M.; Collison, D.; Brechin, E. K.; McInnes, E. J. L. *Inorg. Chem.* **2007**, *46*, 4968. (i) Low, D. M.; Jones, L. F.; Bell, A.; Brechin, E. K.; Mallah, T.; Rivière, E.; Teat, S. J.; McInnes, E. J. L. *Angew. Chem., Int. Ed.* **2003**, *42*, 3781.

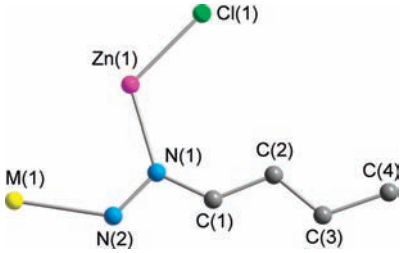

Figure 8. Ball-and-stick representation of the asymmetric units of **1a**, **2a**, **3a**, **3b**, **4b**, and **5a** [M = Zn (**1a**), Fe (**2a**), Co (**3a** and **3b**), Ni (**4b**), Cu (**5a**)]. H atoms and occluded solvent molecules are omitted for clarity.

The N(2)−M(1)−N(2) angles for the central metal atoms do not deviate from right (90°) and straight (180.0°) angles because of the special crystallographic positions of these atoms, leading to a perfect octahedral environment around these metal atoms. Effected by the highly symmetric space group, the M(1)−N(2) distances for the central metal atoms are the same, also indicating the presence of no tetragonal distortion in any of these compounds, as supported by the UV−vis spectroscopic and magnetic studies. It is worth noting that considerable deviations from the ideal octahedral coordination have been previously observed in structurally related copper compounds owing to the Jahn−Teller effect.[5b−d,g,i]

Each set of compounds having either DMF or bromobenzene as occluded solvent molecules shows identical packing arrangements in the crystal lattices. The positions of noncoordinated bromobenzene molecules in **3b** and **4b** can be unequivocally determined from single-crystal data. However, the occluded DMF molecules in **1a**, **2a**, **3a**, and **5a** are highly disordered; thus, it was impossible to refine their positions from the electron density distribution obtained from X-ray diffraction data, even with a reduction of the crystallographic symmetry. Void estimation for **1a**, **2a**, **3a**, and **5a** with *PLATON*/*SQUEEZE*[25] reveals that the average potentially accessible void volume per unit cell volume is 22% and every unit cell contains 16 voids (in which the remaining, unmodeled electron density is located). Each of these voids possesses an average volume of 152.5 Å^3 and might contain a DMF molecule having a volume of 129 Å^3 (calculated from the mass and density of DMF at room temperature). This value is equivalent to two DMF molecules per formula unit, in accordance with the TGA and elemental analysis. Figure 9 illustrates the possible void regions in **5a** that are occupied by noncoordinated DMF molecules.

Magnetic Properties. The magnetism of **2a**, **3a**, **4b**, and **5a** is dominated by the single-ion effects of the central open-shell 3d ions residing in a crystallographically O_h-symmetric [MN_6] environment because intermolecular exchange or dipole−dipole coupling is expected to be low. Both low-field and field-dependent susceptibilities were modeled using our computational framework CONDON, adopting a spin Hamiltonian that incorporates all relevant single-ion effects: interelectronic repulsion (H_{ee}), spin−orbit coupling (H_{so}), the ligand-field effect (H_{lf}), and the Zeeman effect of the applied external field (H_{mag}) (eq 1).[26] The exchange interactions between neighboring molecules in the solid-state lattices are described using a molecular-field approximation, eq 2, where χ'_m represents the single-ion susceptibility contribution and λ_{MF} the molecular-field parameter (positive and negative values of λ_{MF} correlate with ferromagnetic and antiferromagnetic interactions, respectively).

$$\hat{H} = H_{ee} + H_{lf} + H_{so} + H_{mag} \quad (1)$$

$$\chi_m{}^{-1} = \chi'_m{}^{-1}(B, C, \varsigma, B^k_q, J_{ex}) - \lambda_{MF} \quad (2)$$

The parametrization of the octahedral ligand field requires the ligand-field parameter $B^4{}_0$. The corresponding ligand-field operator with reference to the 4-fold rotation axis for the angular part of the wave function then becomes

$$H^{cub}_{lf} = +B^4_0 \sum_{i=1}^{N} C^4_0(i) + B^4_4 \sum_{i=1}^{N} [C^4_4(i) + C^4_{-4}(i)]$$

Because in a cubic system a fixed relationship $B^4_4 = \sqrt{5/14}B^4_0$ exists, only the coefficient $B^4{}_0$ is essential.[27]

The high-spin Fe^{II} d^6 compound **2a** and the Co^{II} d^7 compound **3a** display a continuous decrease in the effective magnetic moment toward low temperatures (Figures 10 and 11). The effective magnetic moment of the cobalt(II) compound **3a** at room temperature is slightly smaller than the value resulting for both spin and orbital momentum (μ_{LS} = 5.20 μ_B), as expected for octahedral high-spin cobalt(II) complexes as a result of spin and first-order orbital contributions.

The Ni^{II} d^8 compound **4b** exhibits nearly temperature-independent μ_{eff} vs T behavior (Figure 12) because of a ligand-field ground state derived from the cubic term $^3A_2$.[28] The effective magnetic moment of **4b** at 290.0 K of 3.16 μ_B is larger than the spin-only value of 2.87 μ_B, as a result of the mixing of excited-state terms into the ground state $^3A_2$ via spin−orbit coupling, which also explains the expected range for octahedral high-spin nickel(II) complexes (S = 1) of 2.8−3.5 μ_B.[29] The susceptibility data display Curie law behavior in the temperature range 20−300 K with a Curie constant $C = 1.569 \times 10^{-5}$ m^3 K mol^{-1} (μ_{eff} = 3.16 μ_B) in very good agreement with the expected value for an isolated paramagnetic Ni^{2+} ion in an octahedral coordination environment. The Brillouin fit to the field-dependent magnetization $M(H)$ at 2.0 K with S = 1 (Figure 12, left inset) yields g = 2.20, which corresponds to the μ_{eff} value at room temperature.

The Cu^{II} d^9 compound **5a** exhibits a virtually temperature-independent effective magnetic moment μ_{eff} = 1.98 and only marginally decreases toward 2 K. However, the appearance of a spin-only system (Figure 13) is caused by the counteracting effects of the ligand-field effect and the spin−orbit coupling in this particular system.

(25) Spek, A. L. *Acta Crystallogr.* **2009**, *D65*, 148.
(26) Schilder, H.; Lueken, H. *J. Magn. Magn. Mater.* **2004**, *281*, 17.
(27) Görller-Walrand, C.; Binnemans, K. Rationalization of Crystal Field Parametrization. In *Handbook on the Physics and Chemistry of Rare Earths*; Gschneidner, K. A., Jr., Eyring, L., Eds.; Elsevier: Amsterdam, The Netherlands, 1996; Vol. *23*, Chapter 155, p 121.
(28) Mabbs, F. E.; Machin, D. J. *Magnetism and Transition Metal Complexes*; Chapman and Hall: London, 1973.
(29) Lueken, H. *Magnetochemie*; Teubner: Stuttgart, Germany, 1999.

Table 2. [d] Selected Bond Lengths (Å) of **1a**, **2a**, **3a**, **3b**, **4b**, and **5a**

	1a, M = Zn	**2a**, M = Fe	**3a**, M = Co	**3b**, M = Co	**4b**, M = Ni	**5a**, M = Cu
Zn(1)−N(1)	2.024(5)	2.022(5)	2.022(5)	2.016(3)	2.009(2)	2.014(7)
M(1)−N(2)	2.183(7)	2.198(8)	2.177(8)	2.178(4)	2.156(3)	2.140(10)
Zn(1)−Cl(1)	2.174(3)	2.168(3)	2.169(3)	2.181(2)	2.1803(15)	2.161(4)
N(1)−N(2)	1.346(7)	1.345(7)	1.348(7)	1.335(3)	1.333(3)	1.352(9)
N(1)−C(1)	1.345(8)	1.341(9)	1.331(8)	1.353(4)	1.357(4)	1.323(11)
C(1)−C(2)	1.414(9)	1.417(10)	1.422(9)	1.412(5)	1.414(4)	1.421(14)
C(2)−C(3)	1.394(9)	1.389(10)	1.393(10)	1.369(5)	1.370(5)	1.411(14)
C(3)−C(4)	1.496(8)	1.491(10)	1.489(10)	1.514(5)	1.509(5)	1.472(14)

[d] Except for **4b** (296 K), single-crystal diffraction data were recorded at T = 293 K. For **1a**, "Zn(1)" should be replaced with "Zn(2)".

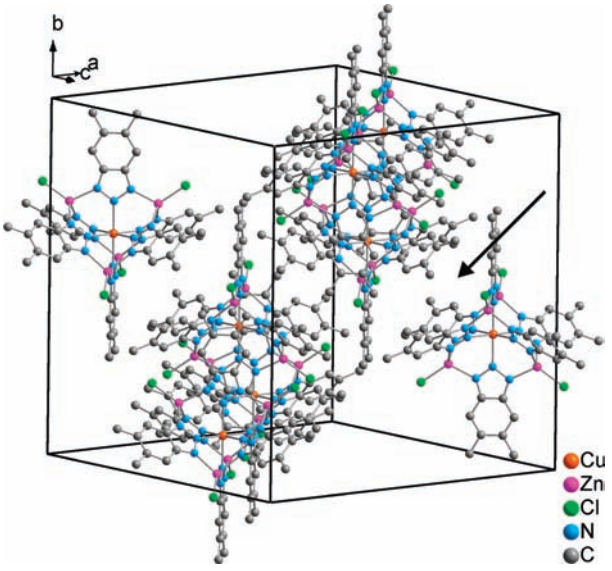

Figure 9. Crystal packing diagram of **5a** in a ball-and-stick representation. The black arrow points to a void region in the crystal lattice that contains a DMF molecule. All H atoms are omitted for clarity.

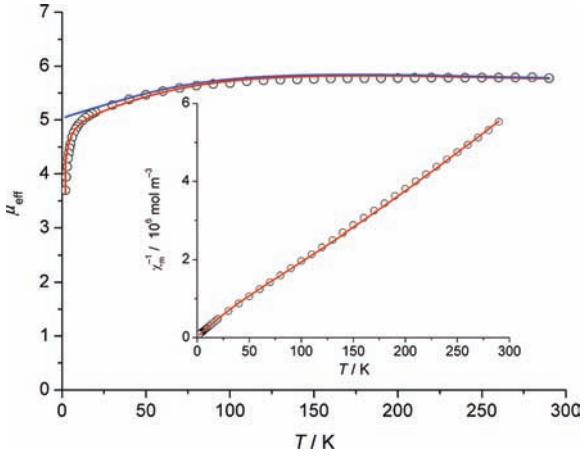

Figure 10. Temperature dependence of the effective magnetic moment μ_{eff} for **2a** at B_0 = 0.1 T. Inset: reciprocal susceptibility at B_0 = 0.1 T. Experimental data: circles. Least-squares fit to the model Hamiltonian (see the text): red line. Single-ion effects (without intermolecular coupling): blue line.

It is worth noting that the ligand-field parameters (Table 3) resulting from the least-squares fits for **2a**, **3a**, **4b**, and **5a** are in overall good agreement with the ligand-field splitting parameters obtained from UV−vis spectroscopy.

Graph Theoretical Representation. The justification to represent the molecular constitution of $[MZn_4X_4(L)_6]$

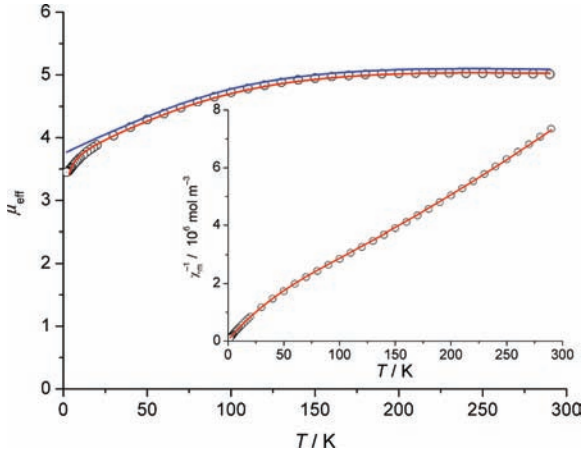

Figure 11. μ_{eff} vs T for **3a** at B_0 = 0.1 T. Inset: reciprocal susceptibility at B_0 = 0.1 T. Experimental data: circles. Least-squares fit to the model Hamiltonian (see the text): red line. Single-ion effects (without intermolecular coupling): blue line.

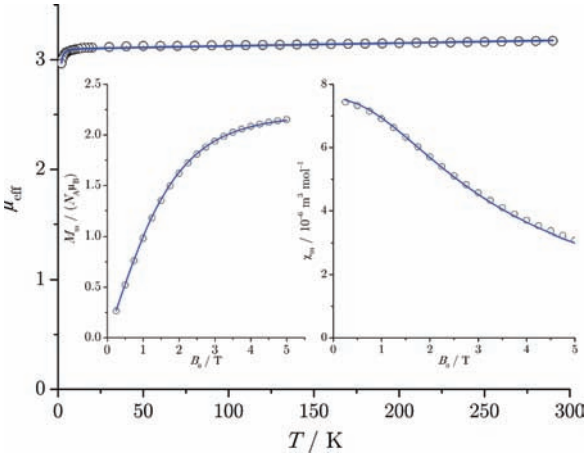

Figure 12. μ_{eff} vs T for **4b** at B_0 = 0.1 T. Insets: M vs B_0 (left) and χ_m vs B_0 (right) at 2.0 K. Experimental data: circles. Least-squares fit to the model Hamiltonian (see the text): blue line.

coordination units by means of a nonplanar graph arises from graph theoretical considerations[30] that prove that these coordination units contain the $K_{3,3}$ graph. In mathematical graph theory, any graph can be classified as planar (those that can be drawn on a plane so that no two edges intersect except at a vertex) or nonplanar (when this cannot be done). The mathematician Casimir Kuratowski was the first to note that all nonplanar graphs contain one of only two basic nonplanar graphs as a subgraph: K_5 (the complete graph on five vertices) and $K_{3,3}$ (the complete, bipartite graph on six

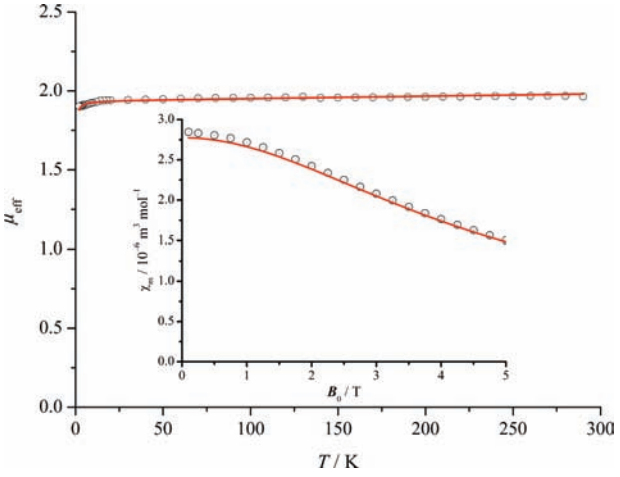

Figure 13. μ_{eff} vs T for **5a** at B_0 = 0.1 T. Inset: χ_m vs B_0 at 2.0 K. Experimental data: circles. Least-squares fit to the model Hamiltonian (see the text): red line.

Table 3. Magnetochemical Analysis Parameters for **2a**, **3a**, **4b**, and **5a**

	2a, M = Fe^{II}	**3a**, M = Co^{II}	**4b**, M = Ni^{II}	**5a**, M = Cu^{II}
B/cm^{-1} (C = 4B)	806	765	715	
ζ/cm^{-1}	420	475	649	820
Dq/cm^{-1} [a]	1140	1200	1085	1430
B_0^4/cm^{-1}	27 300	28 700	20 800	30 100
λ_{MF}/10^5 m^{-3} mol	−0.233	−0.350	*b*	−0.2137
θ/K [c]	−2			−2
SQ/% [d]	1.2	1.5	0.6	0.6

[a] Experimental ligand-field splitting parameter (Dq) from UV−vis spectroscopy; $B_0^4 = 21Dq$. [b] The addition of the molecular-field parameter as a free variable to a least-squares fit did not yield a better fit. [c] Value of the Weiss temperature in a spin-only Curie−Weiss description corresponding to λ_{MF}. [d] SQ = $\{\sum_{i=1}^{n}([\chi_{obs}(i) - \chi_{cal}(i)]/\chi_{obs}(i))^2\}^{1/2}$.

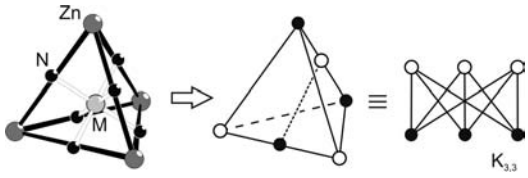

Figure 14. Formal derivation of the $K_{3,3}$ graph, which can be used to represent the connectivity scheme in coordination units of the type $[MZn_4X_4(L)_6]$. The schemes follow recommendations as described in ref 33l.

vertices, three of which connect to each of the other three).[31] As shown in Figure 14, the molecular graph of $[MZn_4X_4(L)_6]$ coordination units, in fact, contains a subgraph of $K_{3,3}$. Accordingly, there is no way to represent $[MZn_4X_4(L)_6]$ coordination units as a planar graph, and thus the pseudoperspective representation shown in Figure 1d seems to be most appropriate for this and related[5] types of coordination compounds.

The graph theoretical representation of the present coordination compounds is interesting in view of the fact that topologically nonplanar molecules are extremely rare in both organic and inorganic chemistry. The molecular graphs of several centrohexacyclic organic (e.g., a centrohexaquinane known as the "Simmons−Paquette molecule",[32] Kuck's centrohexaindanes,[33] and a few ferrocenophanes[34]), metal−organic (e.g., centrohexasexanes such as basic zinc[9] or beryllium[10] carboxylates and related[35] compounds), and inorganic (e.g., centrohexaquadranes such as mixed metal−sulfur cluster anions[36]) species can be reduced to the first Kuratowski graph, K_5. Molecules corresponding to the second Kuratowski graph, $K_{3,3}$, have remained even more scarce than those represented by K_5 graphs. The "Kuratowski cyclophane",[37] Walba's three-rung molecular Möbius ladder,[38] Otsubo's triple-layered naphthalenophane,[39] a cobalt(III) sepulchrate compound,[40] and the recently synthesized cyclohexamantane[41] are among the

(30) (a) Harary, F. In *Chemical Applications of Graph Theory*; Balaban, A. T., Ed.; Academic Press: London, 1976; Chapter 2. (b) Balaban, A. T. *Chemical Applications of Graph Theory*; Academic Press: London, 1976; Chapter 3. (c) Mislow, C. *Bull. Soc. Chim. Belg.* **1977**, *86*, 595. (d) Walba, D. M. *Tetrahedron* **1985**, *41*, 3161. (e) Simon, J. In *Graph Theory and Topology in Chemistry*; King, R. B., Rouvray, D. H., Eds.; Elsevier: Amsterdam, The Netherlands, 1987; p 43. (f) Dietrich-Buchecker, C. O.; Sauvage, J.-P. In *Bioinorganic Chemistry Frontiers*; Dugas, H., Ed.; Springer-Verlag: Berlin, 1991; Vol. *2*, pp 195−248. (g) Liang, C.; Mislow, K. *J. Math. Chem.* **1994**, *15*, 245. (h) Mitchell, D. K.; Chambron, J.-C. *J. Chem. Educ.* **1995**, *72*, 1059. (i) Dodziuk, H. *Modern Conformational Analysis, Methods in Stereochemical Analysis*; Marchand, A. P., Ed.; Wiley-VCH: Weinheim, Germany, 1995.

(31) Kuratowski, C. *Fundam. Math.* **1930**, *15*, 271.

(32) (a) Simmons, H. E., III. Ph.D. Thesis, Harvard University, Boston, MA, 1980. (b) Maggio, J. E. *Tetrahedron Lett.* **1981**, *22*, 287. (c) Kouba, J. K. *J. Am. Chem. Soc.* **1981**, *103*, 1579. (d) Benner, S. A.; Maggio, J. E.; Simmons, H. E., III *J. Am. Chem. Soc.* **1981**, *103*, 1581. (e) Paquette, L. A.; Vazeux, M. *Tetrahedron Lett.* **1981**, *22*, 291.

(33) (a) Kuck, D.; Schuster, A. *Angew. Chem., Int. Ed. Engl.* **1988**, *27*, 1192. (b) Kuck, D.; Paisdor, B.; Gestmann, D. *Angew. Chem., Int. Ed. Engl.* **1994**, *33*, 1251. (c) Kuck, D.; Schuster, A.; Gestmann, D. *J. Chem. Soc., Chem. Commun.* **1994**, 609. (d) Kuck, D.; Schuster, A. *J. Chem. Soc., Perkin Trans. 1* **1995**, 721. (e) Kuck, D. *Synlett* **1996**, 949. (f) Gestmann, D.; Pritzkow, H.; Kuck, D. *Liebigs Ann.* **1996**, 1349. (g) Kuck, D. *Liebigs Ann. Recl.* **1997**, 1043. (h) Kuck, D.; Krause, R. A.; Gestmann, D.; Posteher, F.; Schuster, A. *Tetrahedron* **1998**, *54*, 5247. (i) Kuck, D. The Centropolyindanes and Related Centro-Fused Polycyclic Organic Compounds. In *Carbon Rich Compounds I, Topics in Current Chemistry*; de Meijere, A., Ed.; Springer: Heidelberg, Germany, 1998; Vol. *196*, pp 168−208. (j) Kuck, D. Benzoannelated Fenestranes. In *Advances in Theoretically Interesting Molecules*; Thummel, R. P., Ed.; JAI Press: Greenwich, London, 1998. (k) Harig, M.; Kuck, D. *Eur. J. Org. Chem.* **2006**, 1647. (l) Kuck, D. Molecules with Nonstandard Topological Properties: Centrohexaindane, Kuratowski's Cyclophane and Other Graph-theoretically Nonplanar Molecules. In *Strained Hydrocarbons. Beyond the Van't Hoff and LeBel Hypothesis*; Dodziuk, H., Ed.; Wiley-VCH: Weinheim, Germany, 2009; Chapter 9, pp 425−447.

(34) (a) Hisatome, M.; Watanabe, N.; Sakamoto, T.; Yamakawa, K. *J. Organomet. Chem.* **1977**, *125*, 79. (b) Hisatome, M.; Kawaziri, Y.; Yamakawa, K. *Tetrahedron Lett.* **1979**, 1777. (c) Hisatome, M.; Kawaziri, Y.; Yamakawa, K. *Tetrahedron Lett.* **1982**, 1713.

(35) (a) Burn, A. J.; Smith, G. W. *J. Chem. Soc., Chem. Commun.* **1965**, 394. (b) Scattergood, C. D.; Bonney, P. G.; Slater, J. M.; Garner, C. D.; Clegg, W. *J. Chem. Soc., Chem. Commun.* **1987**, 1749. (c) Müller, A.; Krickemeyer, E.; Hildebrand, A.; Bögge, H.; Schneider, K.; Lemke, M. *J. Chem. Soc., Chem. Commun.* **1991**, 1685. (d) Bernès, S.; Sécheresse, F.; Jeannin, Y. *Inorg. Chim. Acta* **1992**, *191*, 11. (e) Jeannin, Y.; Sécheresse, F.; Bernès, S.; Robert, F. *Inorg. Chim. Acta* **1992**, *198−200*, 493.

(36) (a) Scattergood, C. D.; Bonney, P. G.; Slater, J. M.; Garner, C. D.; Clegg, W. *J. Chem. Soc., Chem. Commun.* **1987**, 1749. (b) Müller, A.; Krickemeyer, E.; Hildebrand, A.; Bögge, H.; Schneider, K.; Lemke, M. *J. Chem. Soc., Chem. Commun.* **1991**, 1685. (c) Bernès, S.; Sécheresse, F.; Jeannin, Y. *Inorg. Chim. Acta* **1992**, *191*, 11. (d) Jeannin, Y.; Sécheresse, F.; Bernès, S.; Robert, F. *Inorg. Chim. Acta* **1992**, *198−200*, 493.

(37) Chen, C.-T.; Gantzel, P.; Siegel, J. S.; Baldrigde, K. K.; English, R. B.; Ho, D. M. *Angew. Chem., Int. Ed. Engl.* **1988**, *34*, 2657.

(38) Walba, D. M.; Richards, R. M.; Haltiwanger, R. C. *J. Am. Chem. Soc.* **1982**, *104*, 3219.

(39) Otsubo, T.; Ogura, F.; Misumi, S. *Tetrahedron Lett.* **1983**, *24*, 4851.

(40) (a) Creaser, I. I.; Harrowfield, J. M.; Herlt, A. J.; Sargeson, A. M.; Springborg, J.; Geue, R. J.; Snow, M. R. *J. Am. Chem. Soc.* **1977**, *99*, 3181. (b) Creaser, I. I.; Geue, R. J.; Harrowfield, G. M.; Herlt, A. J.; Sargeson, A. M.; Snow, M. R.; Springborg, J. *J. Am. Chem. Soc.* **1982**, *104*, 6016.

(41) Dahl, J. E. P.; Moldowan, J. M.; Peakman, T. M.; Clardy, J. C.; Lobkovsky, E.; Olmstead, M. M.; May, P. W.; Davis, T. J.; Steeds, J. W.; Peters, K. E.; Pepper, A.; Ekuan, A.; Carlson, R. M. K. *Angew. Chem., Int. Ed.* **2003**, *42*, 2040.

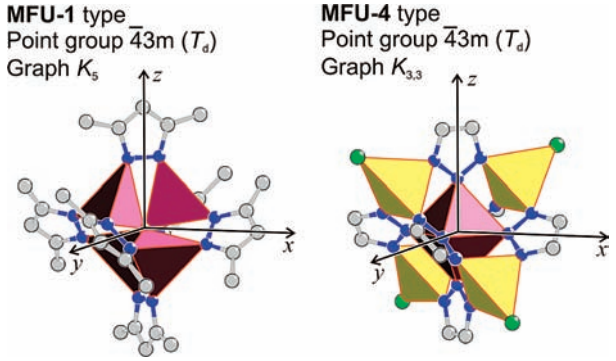

Figure 15. Comparative structural features of the coordination units found in **MFU-1** (left) and **MFU-4** (right) (C, gray; N, blue; Cl, green; Zn, yellow; redox-active metal centers M, pink).

few molecules with nonplanar $K_{3,3}$ topology. The molecular graphs of polynuclear metal carbonyl carbide clusters[42] and several other[43] molecules are reducible to either K_5 or $K_{3,3}$ graphs by suitable deletions or contractions and, hence, may be considered as topologically nonplanar.

From a topological point of view, all of the above-mentioned organic, metal−organic, or inorganic centrohexacyclic compounds are isostructural to the fundamental SBUs of **MOF-5** and **MFU-1** types of frameworks. Focusing only on the metal−organic compounds, the coordination units $[MZn_4X_4(L)_6]$ and the basic zinc or beryllium carboxylates represent the only two classes of minimum nonplanar coordination units having T_d point group symmetry, from which highly regular three-dimensional porous frameworks can be constructed in a predictable and systematic fashion (see Figure 15). Therefore, it can be safely predicted that the chemistry of such coordination units and their integration into MOF networks will develop rapidly in the near future. Moreover, and in sharp contrast with the molecular coordination units featured by **MOF-5** and related networks, the present Kuratowski-type coordination units are likewise stable and can be easily prepared at a multigram scale, which opens up possibilities for the rational systematic design of the corresponding frameworks as well as for optimization of their functional properties. Notably, the Kuratowski type of $K_{3,3}$ nodes are interconnected with the planar organic linkers in a stereochemically predefined manner. In contrast, the K_5 nodes are cross-linked via single-bonded types of linkages, leading to the extensive formation of supramolecular isomers of the same basic framework topology.

(42) (a) Braye, E. H.; Dahl, L. F.; Hübel, W.; Wampler, D. L. *J. Am. Chem. Soc.* **1962**, *84*, 4633. (b) Jackson, P. F.; Johnson, B. F. G.; Lewis, J.; Nicholls, J. N. *J. Chem. Soc., Chem. Commun.* **1980**, 564. (c) Lewis, J.; Johnson, B. F. G. *Pure Appl. Chem.* **1982**, *54*, 97.

(43) (a) Momenteau, M.; Mispelter, J.; Loock, B.; Bisagni, E. *J. Chem. Soc., Perkin Trans. 1* **1983**, 189. (b) Okuno, Y.; Uoto, K.; Sasaki, Y.; Yonemitsu, O.; Tomohiro, T. *J. Chem. Soc., Chem. Commun.* **1987**, 874. (c) Barigelletti, F.; Cola, L. D.; Balzani, V.; Belser, P.; Zelewsky, A. V.; Vögtle, F.; Ebmeyer, F.; Grammenudi, S. *J. Am. Chem. Soc.* **1989**, *111*, 4662. (d) Bour, J. J.; Berg, W. V. D.; Schlebos, P. P. J.; Kanters, R. P. F.; Schoondergang, M. F. J.; Bosman, W. P.; Smits, J. M. M.; Beurskens, P. T.; Steggerda, J. J.; Sluis, P. V. D. *Inorg. Chem.* **1990**, *29*, 2971. (e) Hegetschweiler, K.; Schmalle, H.; Streit, H. M.; Schneider, W. *Inorg. Chem.* **1990**, *29*, 3625.

Conclusions

We have demonstrated the successful design, syntheses, and in-depth characterization of a novel series of readily available, thermally and solvolytically stable, homo- and heteropentanuclear compounds that represent discrete molecular analogues of the SBU of the metal−organic framework **MFU-4**. The Kuratowski-type coordination compounds $[M^{II}Zn_4Cl_4(Me_2bta)_6]$ (M^{II} = Zn, Fe, Co, Ni, or Cu) can be readily synthesized at multigram scale. Single-crystal X-ray diffraction data reveal that the open-shell metal ions in all heteropentanuclear complexes are in high-spin state without undergoing any Jahn−Teller distortion, which has been further verified by electronic spectroscopy and magnetic measurements. TGA and TOF-MS analyses exhibit exceptionally high thermal and solvolytic stability of the compounds, respectively. These properties, in combination with the presence of coordinatively unsaturated Zn sites and the redox-active open-shell metal ions, would make them model catalysts in homogeneous Lewis acid and redox-catalyzed reactions for the structurally related **MFU-4** type of heterogeneous catalysts. Moreover, such compounds might display interesting combinations of useful properties such as luminescence or reversible electron transfer. Finally, the present compounds represent a rare class of topologically nonplanar building units having T_d point group symmetry and $K_{3,3}$ as the molecular graph, in analogy of which a large number of cubic porous frameworks can be constructed in a predictable and systematic fashion. Investigations in this direction are in progress in our laboratory and will be reported in due course.

Acknowledgment. Financial support from the German Research Foundation (DFG Priority Program 1362 "Porous Metal−Organic Frameworks", VO 829/5-1) is gratefully acknowledged. M.T. is grateful to the Landesgraduiertenförderung Baden-Württemberg for financial support. The authors thank Prof. D. Kuck (University of Bielefeld, Bielefeld, Germany) for fruitful discussions about graph theoretical applications. P.K. thanks the RWTH Aachen University for a Seed Fund.

Supporting Information Available: PXRD patterns, FT-IR spectra, TGA curves, EDX spectra, TOF-MS spectra, optical micrographs, a detailed view of the asymmetric units, tables containing IR frequencies, elemental and ICP-AES analyses, atomic coordinates, bond lengths and angles, and anisotropic displacement parameters, and a CIF file. This material is available free of charge via the Internet at http://pubs.acs.org.